Gen. Math. Notes, Vol. 20, No. 2, February 2014, pp.22-49

ISSN 2219-7184; Copyright ©ICSRS Publication, 2014

www.i-csrs.org

Available free online at http://www.geman.in

Numerical Study of a Non-Linear Peristaltic Transport: Application of Adomian Decomposition Method(ADM)

Kh. S. Mekheimer[1], K.A. Hemada[2], K.R. Raslan[3], R.E. Abo-Elkhair[4] and A.M.A. Moawad[5]

[1]Mathematics & Statistics Department, Faculty of Science
Taif University, Hawia 888, Taif, KSA
E-mail: kh_mekheimer@yahoo.com
[2,3,4,5]Mathematical Department, Faculty of Science (Men)
Al-Azhar University, Nasr City 11884, Cairo, Egypt
[2]E-mail:hemidakamal@yahoo.com
[3]E-mail:kamal_raslan@yahoo.com
[4]E-mail:elkhair33@yahoo.com
[5]E-mail:ali_moawad2008@yahoo.com

(Received: 8-11-13 / Accepted: 15-12-13)

Abstract

The aim of this problem is to study the peristaltic motion of a Newtonian, homogenous and incompressible viscous fluid in a two dimensional channel by using Adomian Decomposition Method. The expressions for stream function, velocity and vorticity are obtained without any approximation for the governing equations and also for the choice of the problem parameters values, but we used Adomian Decomposition Method as approximated one. The effects for arbitrary values of wave number (α), amplitude ratio (ϕ) and Reynolds number (R_e) on flow characteristics are studied in detail.

Keywords: *ADM, Peristaltic transport, Numerical Study.*

1 Introduction

When a progressive wave resulting from area contraction and expansion of an extensible tube propagates along the length of the tube, a fluid contained in the tube is mixed and transported in the direction of the wave propagation as if it were squeezed out by the moving wall. This phenomenon, called "peristalsis", is an inherent property of any tubular organ of the human body such as the ureter, the gastro-intestinal tract, or the small blood vessels. In the last decades the mechanism of this mixing and transporting peristaltic motion has acquired general interest in the field of hydrodynamics and a number of studies have been undertaken with respect to peristaltic flows by applying a simple hydrodynamic model represented by sinusoidal waves. Some of them are summarized in the review by Jaffrin & Shapiro (1971) [1]. Since these studies have been developed in connection with the function of organs of the human body, many of them have been concerned with the flow within a range of small Reynolds numbers. Moreover, peristaltic pumping has been quite recently utilized for the transport of such fluids as blood, slurries, corrosive fluids, and it is desirable to prevent them from coming into contact with the mechanical parts of the pump. So it is necessary that the peristaltic flow at moderate Reynolds numbers should be analyzed.

In the range of finite Reynolds number, a theoretical analysis of the peristaltic flow is extremely difficult because of the nonlinearity due to the interaction between the moving wall and the flow field.Fung & Yih (1968)[2] first performed a study of peristaltic flow including small nonlinear effects. They treated the case of a two-dimensional channel with a small ratio of amplitude to wavelength of the peristaltic wave, and their analysis was based upon perturbations of the ratio of wave amplitude to mean channel width. Shapiro, Jaffrin & Weinberg (1969)[3] obtained a linear solution of peristaltic flow by considering the limiting case in which the wavelength was infinite and the fluid inertia could be neglected, and by applying Stokes' approximation to the flow. This linear solution was modified later by Jaffrin (1973)[4] in his consideration of small nonlinear effects. He made a perturbation analysis so as to obtain the series solutions for both the case of long wavelength at zero Reynolds number and the case of small Reynolds number at infinite wavelength. The applicable range of these series solutions was studied through a comparison with experimental results (Weinberg, Eckstein & Shapiro 1971)[5]. For the limiting case of large Reynolds number with small amplitude and long wavelength, Hanin (1968)[6] analyzed the flow by applying the boundary-layer equation, and Ayukawa, Kawai & Kimura (1981)[7] obtained experimental results as well as an approximate solution of potential flow on the basis of source distributions. In these two works, the peristaltic pumping was investigated with reference to engineering applications. On the other hand, with respect

to numerical investigations, we have the analyses of Tong & Vawter (1972)[8] and Brown & Hung(1977)[9]. The former uses the finite-element method that is available for the case of large amplitude, and the latter applies the finite-difference method by employing orthogonal curvilinear coordinates. Recently Kh. S. Mekheimer & et al. ([10]-[13]) obtained a linear solution of peristaltic flow by considering the limiting case in which the wavelength was infinite. But each of them has its disadvantage in requiring enormous and complicated calculations and/or a restriction on the geometry of the calculating region. In this paper, the Navier-Stokes equations are solved numerically by using Adomian Decomposition Method on the peristaltic flow induced by an infinite train of sinusoidal waves in a two-dimensional channel.The second section will give brief summary of the solution method which will be used. But the third section will explain in detail the form of the problem and find a solution by using Adomian Decomposition Method to get a stream function, velocity and vorticity of the fluid and in the fourth section, we will discuss in detail the results we have obtained and The effects of wave number (α), amplitude ratio (ϕ) and Reynolds number (R_e) on flow characteristics .

2 Adomian Decomposition Method(ADM)([14]-[18])

In this section we will discuss the Adomian Decomposition Method. The Adomian Decomposition Method has been receiving much attention in recent years in applied mechanics in general, and in the area of series solutions in particular. The method proved to be powerful, effective, and can easily handle a wide class of linear or nonlinear, ordinary or partial differential equations, and linear or nonlinear integral equations. The decomposition method demonstrates fast convergence of the solution and therefore provides several significant advantages. The Adomian Decomposition Method was introduced and developed by George Adomian in and is well addressed in the literature. A considerable amount of research work has been invested recently in applying this method to a wide class of linear and nonlinear ordinary differential equations, partial differential equations and integral equations as well. The Adomian Decomposition Method consists of decomposing the unknown function $u(x, y)$ of any equation into a sum of an infinite number of components defined by the decomposition series:

$$u(x, y) = \sum_{n=0}^{\infty} u_n(x, y), \tag{1}$$

where the components $u_n(x, y)$ $(n \geq 0)$ are to be determined in a recursive manner. The decomposition method concerns itself with finding the com-

ponents $(u_0, u_1, u_2, \cdots)$ individually. As will be seen through the text, the determination of these components can be achieved in an easily way through a relation that usually involve simple integrals. In this study, we solve for $(L_y(u))$, hence the other linear operators, Simply become R operator in the partial differential equation as follows:

$$L_y(u) + R(u) + N(u) = g(x, y), \tag{2}$$

where $N(u)$ represents the nonlinear term and $L_y(*) = \frac{\partial^n(*)}{\partial y^n}$, therefore:

$$L_y(u) = -R(u) - N(u) + g(x, y). \tag{3}$$

Then we operate both sides the inverse operator (assuming it exists) which is an n-fold integration operator from 0 to y, since

$$L_y^{-1}(*) = \underbrace{\int_0^y (*)dy}_{n-times},$$

so:

$$L_y^{-1}(L_y(u)) = -L_y^{-1}(R(u)) - L_y^{-1}(N(u)) + L_y^{-1}(g(x, y)). \tag{4}$$

Then, we get:

$$L_y^{-1}(L_y(u)) = u - \Phi_y,$$

where

$$\Phi_y = \sum_{j=0}^{n-1} \frac{K_j(x)y^j}{j!},$$

and $K_j(x)$ are the integration constants which are evaluated from the given conditions, so:

$$u(x, y) = \sum_{j=0}^{n-1} \frac{K_j(x)y^j}{j!} + L_y^{-1}(g(x, y)) - L_y^{-1}(R(u)) - L_y^{-1}(N(u)). \tag{5}$$

In the use of this method, the solution of the partial differential equation is written as:(1), where u_0 is a function involving the initial (or boundary) conditions, the forcing function $g(x, y)$ and integral constants. The other components of u are determined by recursive relation. The nonlinear term $N(u)$, such as $(u^2, u^3, \sin[u], \cdots)$, etc. can be expressed by infinite series of the so-called Adomian polynomials A_n given in the form

$$N(u) = \sum_{n=0}^{\infty} A_n(u_0, u_1, u_2, \cdots, u_n), \tag{6}$$

where A_n are specially generated Adomian polynomials for the specific nonlinearity. The Adomian polynomials A_n for nonlinear term $N(u)$ can be evaluated by using the following expression

$$A_n = \frac{1}{n!}\frac{d^n}{d\zeta^n}(N(\sum_{i=0}^{n}\zeta^i u_i))|_{\zeta=0}, \quad n \geq 0. \tag{7}$$

So the solution can now be written as:

$$u(x,y) = \sum_{n=0}^{\infty} u_n = \sum_{j=0}^{n-1}\frac{K_j(x)y^j}{j!} + L^{-1}(g(x,y)) - L^{-1}(R(\sum_{n=0}^{\infty}u_n)) - L^{-1}(\sum_{n=0}^{\infty}A_n)), \tag{8}$$

where the first two terms from the last equation are identified as u_0 in the assumed decomposition series and the other terms represent the components after u_0. Then we get the following recursive relation:

$$\begin{aligned} u_0 &= \sum_{j=0}^{n-1}\frac{K_j(x)y^j}{j!} + L^{-1}(g(x,y)), \\ u_{n+1} &= -L^{-1}(R(u_n)) - L^{-1}(A_n), \quad n \geq 0. \end{aligned} \tag{9}$$

From which all components of the decomposition are identified and computed.

3 Statement of Physical Model

A Newtonian, homogenous and incompressible viscous fluid with no restriction either on the geometry or on non-linearity is considered. In the fixed frame (X,Y) the central axis of a two dimensional channel is taken along the X-axis (see figure 1). The wall of the domain is defined by

$$H(X,T) = h - \epsilon\cos[\frac{2\pi}{\lambda}(X - CT)], \tag{10}$$

where, T is time, ϵ is the wave amplitude, h is the mean distance of the wall from the central axis, λ is the wave length and C is the velocity with which the infinite train of sinusoidal wave progresses along the wall in the positive X-direction. The flow which is unsteady in the fixed frame (X,Y) appears steady in the moving frame (x', y') which travels in the positive X-direction with velocity "C".

The relations between the two frames are:

$$x' = X - CT, \qquad y' = Y, \qquad u' = U - C, \qquad v' = V. \tag{11}$$

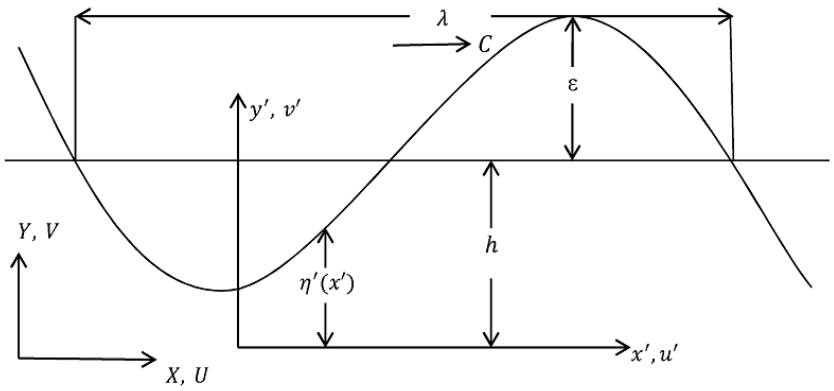

Figure 1: Geometry of two-dimensional peristaltic channel

Where (U,V) and (u',v') are components of velocity in the fixed and moving frames respectively. In the fixed frame the equations governing the flow (with pressure "P ", viscosity "μ" and density "ρ") are:

$$\frac{\partial U}{\partial X}+\frac{\partial V}{\partial Y}=0, \tag{12}$$

$$\rho[\frac{DU}{DT}]=\rho[\frac{\partial U}{\partial T}+U\frac{\partial U}{\partial X}+V\frac{\partial U}{\partial Y}]=-\frac{\partial P}{\partial X}+\mu[\frac{\partial^2 U}{\partial X^2}+\frac{\partial^2 U}{\partial Y^2}], \tag{13}$$

and

$$\rho[\frac{DV}{DT}]=\rho[\frac{\partial V}{\partial T}+U\frac{\partial V}{\partial X}+V\frac{\partial V}{\partial Y}]=-\frac{\partial P}{\partial Y}+\mu[\frac{\partial^2 V}{\partial X^2}+\frac{\partial^2 V}{\partial Y^2}], \tag{14}$$

and the boundary conditions are:

$$\begin{aligned} &V=0, \qquad \frac{\partial U}{\partial Y}=0, \qquad \text{at } Y=0,\\ &U=0, \qquad V=\frac{dH}{dT}=-\frac{2\pi C}{\lambda}\epsilon\sin[\frac{2\pi}{\lambda}(X-CT)] \qquad \text{at } Y=H. \end{aligned} \tag{15}$$

The stream function Ψ and the vorticity Ω in the fixed frame are introduced as:

$$U-C=\frac{\partial \Psi}{\partial Y}, \qquad V=-\frac{\partial \Psi}{\partial X}, \qquad \Omega=\frac{\partial V}{\partial X}-\frac{\partial U}{\partial Y}, \tag{16}$$

and in the moving frame (x',y') the stream function ψ' and vorticity ω' are defined by

$$u'=\frac{\partial \psi'}{\partial y'}, \qquad v'=-\frac{\partial \psi'}{\partial x'}, \qquad \omega'=\frac{\partial v'}{\partial x'}-\frac{\partial u'}{\partial y'}. \tag{17}$$

Using equations (11) in [(12) to (15)], we obtain the governing equations in the moving frame as:

$$\frac{\partial u'}{\partial x'} + \frac{\partial v'}{\partial y'} = 0, \tag{18}$$

$$\rho[u'\frac{\partial u'}{\partial x'} + v'\frac{\partial u'}{\partial y'}] = -\frac{\partial p'}{\partial x'} + \mu[\frac{\partial^2 u'}{\partial x'^2} + \frac{\partial^2 u'}{\partial y'^2}], \tag{19}$$

and

$$\rho[u'\frac{\partial v'}{\partial x'} + v'\frac{\partial v'}{\partial y'}] = -\frac{\partial p'}{\partial y'} + \mu[\frac{\partial^2 v'}{\partial x'^2} + \frac{\partial^2 v'}{\partial y'^2}]. \tag{20}$$

Also, the configuration of the peristaltic wall can be represented by:

$$\eta'(x') = h - \epsilon\cos[\frac{2\pi}{\lambda}x'], \tag{21}$$

and the no-slip condition or the symmetry condition on the planes $y' = 0$ and $y' = \eta'(x')$ can be expressed as follows:

$$\begin{aligned} &v' = 0, \qquad \frac{\partial u'}{\partial y'} = 0, \qquad \text{at } y' = 0, \\ &u' = -C, \qquad v' = -\frac{2\pi C}{\lambda}\epsilon\sin[\frac{2\pi}{\lambda}x'], \qquad \text{at } y' = \eta'(x'). \end{aligned} \tag{22}$$

Moreover, since the both planes $y' = 0$ and $y' = \eta'(x')$ constitute the streamlines in the wave frame, the flow rate ($q' = \int u'dy'$) in the wave frame is constant at all cross-sections of the channel. Thus the following equation can be obtained as:

$$\psi' = 0, \qquad \text{at } y' = 0, \qquad \psi' = q', \qquad \text{at } y' = \eta'(x'). \tag{23}$$

The dimensionless variables defined by:

$$\begin{aligned} &x = \frac{x'}{\lambda}, \qquad y = \frac{y'}{h}, \qquad u = \frac{u'}{C}, \\ &v = \frac{\lambda}{Ch}v', \qquad \psi = \frac{\psi'}{Ch}, \qquad \omega = \frac{h}{C}\omega', \\ &q = \frac{q'}{Ch}, \qquad p = \frac{h^2}{\mu c\lambda}p', \qquad \eta = \frac{\eta'}{h}, \end{aligned} \tag{24}$$

will be used; and the amplitude ratio "ϕ", the wave number "α", and the Reynolds number "R_e", are defined by

$$\alpha = \frac{h}{\lambda}, \qquad R_e = \frac{\rho Ch}{\mu}, \qquad \phi = \frac{\epsilon}{h}. \tag{25}$$

Equation of motion and boundary conditions in the dimensionless form become:

$$\frac{\partial u}{\partial x}+\frac{\partial v}{\partial y}=0, \tag{26}$$

$$R_e\alpha[u\frac{\partial u}{\partial x}+v\frac{\partial u}{\partial y}]=-\frac{\partial p}{\partial x}+[\alpha^2\frac{\partial^2 u}{\partial x^2}+\frac{\partial^2 u}{\partial y^2}], \tag{27}$$

and

$$R_e\alpha^3[u\frac{\partial v}{\partial x}+v\frac{\partial v}{\partial y}]=-\frac{\partial p}{\partial y}+\alpha^2[\alpha^2\frac{\partial^2 v}{\partial x^2}+\frac{\partial^2 v}{\partial y^2}]. \tag{28}$$

Also, the configuration of the peristaltic wall can be represented by:

$$\eta(x)=1-\phi\cos[2\pi x], \tag{29}$$

and the no-slip condition or the symmetry condition on the planes $y=0$ and $y=\eta(x)$ can be expressed as follows:

$$\begin{aligned} &v=0, \qquad \frac{\partial u}{\partial y}=0, \qquad \psi=0 \qquad \text{at } y=0,\\ &u=-1, \qquad v=-2\pi\phi\sin[2\pi x], \qquad \psi=q \qquad \text{at } y=\eta(x), \end{aligned} \tag{30}$$

and the stream function ψ and vorticity ω are defined by:

$$u=\frac{\partial \psi}{\partial y}, \qquad v=-\frac{\partial \psi}{\partial x}, \qquad \omega=\alpha^2\frac{\partial v}{\partial x}-\frac{\partial u}{\partial y}. \tag{31}$$

By eliminating the pressure from equations (27) and (28), we get:

$$\begin{aligned} R_e\alpha[u(\frac{\partial^2 u}{\partial x\partial y}-\alpha^2\frac{\partial^2 v}{\partial x^2})+v(\frac{\partial^2 u}{\partial y^2}-\alpha^2\frac{\partial^2 v}{\partial x\partial y})]&\\ =[(\alpha^2\frac{\partial^2}{\partial x^2}+\frac{\partial^2}{\partial y^2})(\frac{\partial u}{\partial y}-\alpha^2\frac{\partial v}{\partial x})]&. \end{aligned} \tag{32}$$

Using equations (31) in [(30) and (32)], we get the governing equations and boundary conditions as:

$$\begin{aligned} R_e\alpha[(\frac{\partial \psi}{\partial y})(\frac{\partial^3\psi}{\partial x\partial y^2}+\alpha^2\frac{\partial^3\psi}{\partial x^3})-(\frac{\partial \psi}{\partial x})(\frac{\partial^3\psi}{\partial y^3}+\alpha^2\frac{\partial^3\psi}{\partial x^2\partial y})]&\\ =[(\alpha^2\frac{\partial^2}{\partial x^2}+\frac{\partial^2}{\partial y^2})(\frac{\partial^2\psi}{\partial y^2}+\alpha^2\frac{\partial^2\psi}{\partial x^2})]&. \end{aligned} \tag{33}$$

For simplify, we get:

$$\begin{aligned}\frac{\partial^4\psi}{\partial y^4} =&R_e\alpha[(\frac{\partial\psi}{\partial y})(\frac{\partial^3\psi}{\partial x\partial y^2}+\alpha^2\frac{\partial^3\psi}{\partial x^3})-(\frac{\partial\psi}{\partial x})(\frac{\partial^3\psi}{\partial y^3}+\alpha^2\frac{\partial^3\psi}{\partial x^2\partial y})]\\ &-[\alpha^4\frac{\partial^4\psi}{\partial x^4}+2\alpha^2\frac{\partial^4\psi}{\partial x^2\partial y^2}],\end{aligned} \tag{34}$$

and the no-slip condition or the symmetry condition on the planes $y=0$ and $y=\eta(x)$ can be expressed as follows:

$$\begin{aligned}&\psi=0, \qquad \frac{\partial^2\psi}{\partial y^2}=0, \qquad \frac{\partial\psi}{\partial x}=0 \qquad \text{at } y=0,\\ &\psi=q, \qquad \frac{\partial\psi}{\partial y}=-1, \qquad \frac{\partial\psi}{\partial x}=-2\pi\phi\sin[2\pi x] \qquad \text{at } y=\eta(x).\end{aligned} \tag{35}$$

4 ADM Solution

For the solution of equation (34) with the boundary conditions (35) , we use Adomian Decomposition Method, we write equation (34) in operator form

$$\begin{aligned}\psi =&L_y^{-1}(R_e\alpha[(\frac{\partial\psi}{\partial y})(\frac{\partial^3\psi}{\partial x\partial y^2}+\alpha^2\frac{\partial^3\psi}{\partial x^3})-(\frac{\partial\psi}{\partial x})(\frac{\partial^3\psi}{\partial y^3}+\alpha^2\frac{\partial^3\psi}{\partial x^2\partial y})])\\ &-L_y^{-1}([\alpha^4\frac{\partial^4\psi}{\partial x^4}+2\alpha^2\frac{\partial^4\psi}{\partial x^2\partial y^2}]).\end{aligned} \tag{36}$$

Since

$$L_y^{-1}(*)=\underbrace{\int_0^y(*)dy}_{4\text{ - times}},$$

So, Now we can decompose ψ as:

$$\psi=\sum_{n=0}^{\infty}\psi_n. \tag{37}$$

Substituting ψ into equation (36), and using the boundary equations (35), then we get the following recursive relation:

$$\begin{aligned}&\psi_0=y\left(\frac{\eta(x)+3q}{2\eta(x)}\right)-y^3\left(\frac{\eta(x)+q}{2\eta^3(x)}\right),\\ &\psi_{(n\geq1)}=\Phi_{y,n}+L_y^{-1}(R_e\alpha[(\frac{\partial\psi_{n-1}}{\partial y})(\frac{\partial^3\psi_{n-1}}{\partial x\partial y^2}+\alpha^2\frac{\partial^3\psi_{n-1}}{\partial x^3})\\ &-(\frac{\partial\psi_{n-1}}{\partial x})(\frac{\partial^3\psi_{n-1}}{\partial y^3}+\alpha^2\frac{\partial^3\psi_{n-1}}{\partial x^2\partial y})])-L_y^{-1}([\alpha^4\frac{\partial^4\psi_{n-1}}{\partial x^4}+2\alpha^2\frac{\partial^4\psi_{n-1}}{\partial x^2\partial y^2}]),\\ &\text{since}\qquad \Phi_{y,n}=c_{0,n}(x)+yc_{1,n}(x)+y^2c_{2,n}(x)+y^3c_{3,n}(x),\end{aligned} \tag{38}$$

where $c_{0,n}$. $c_{1,n}$, $c_{2,n}$, $c_{3,n}$ are the integration constants which are evaluated from the given conditions.
Then the solution of the stream function written as:

$$\psi = \sum_{n=0}^{\infty} \psi_n = \psi_0 + \psi_1 + \psi_2 + \cdots$$
$$= y\left(\frac{\eta(x)+3q}{2\eta(x)}\right) - y^3\left(\frac{\eta(x)+q}{2\eta^3(x)}\right) - \frac{1}{20160\eta^9(x)} y\alpha(y^2-\eta^2(x))^2[R_e(120q^2y^4$$
$$\times \alpha^2\eta'^3(x) + 15qy^4\alpha^2\eta(x)\eta'(x)(14\eta'^2(x) - 9q\eta''(x)) + 6\alpha^2\eta^8(x)\eta^{(3)} + 3\alpha^2$$
$$\times \eta^7(x)(2\eta'(x)\eta''(x) - 5q\eta^{(3)}(x)) + \eta^5(x)(\eta'(x)(-792q - \alpha^2(54q\eta'^2(x)+$$
$$(783q^2 + 32y^2)\eta''(x))) - 58qy^2\alpha^2\eta^{(3)}(x)) + y^2\eta^3(x)(2\eta'(x)(30q(6 - 5\alpha^2\eta'^2(x))$$
$$+ (243q^2 - 35y^2)\alpha^2\eta''(x)) + 25qy^2\alpha^2\eta^{(3)}(x)) + 3y^2\eta^2(x)(4(-34q^2 + 5y^2)\alpha^2$$
$$\times \eta'^3(x) + 2q\eta'(x)(36q - 35y^2\alpha^2\eta''(x)) + 5q^2y^2\alpha^2\eta^{(3)}(x)) + 2\eta^4(x)(6\eta'(x)$$
$$\times (-90q^2 + 12y^2 + \alpha^2((48q^2 - 2y^2)\eta'^2(x) + 25qy^2\eta''(x))) + y^2(-39q^2 + 5y^2)$$
$$\times \alpha^2\eta^{(3)}(x)) + \eta^6(x)(54\eta'(x)(-4 + \alpha^2(-2\eta'^2(x) + q\eta''(x))) + (270q^2 + 8y^2)$$
$$\times \alpha^2\eta^{(3)}(x))) + 12\alpha^2(-360qy^2\alpha^2\eta'^4(x) - 120y^2\alpha^2\eta(x)\eta'^2(x)(\eta'^2(x) - 3q\eta''(x))$$
$$- 12\eta^2(x)(18q\alpha^2\eta'^4(x) + 3qy^2\alpha^2\eta''^2(x) + 12\eta'^2(x)(7q - y^2\alpha^2\eta''(x)) + 4qy^2\alpha^2$$
$$\times \eta'(x)\eta^{(3)}(x)) + 4\alpha^2\eta^6(x)\eta^{(4)}(x) - 3\alpha^2\eta^5(x)(12\eta''^2(x) + 16\eta'(x)\eta^{(3)(x)} + 5q$$
$$\times \eta^{(4)}(x)) - 3\eta^3(x)(80\alpha^2\eta'^4(x) - 84q\eta''(x) + 12\eta'^2(x)(14 + q\alpha^2\eta''(x)) + 8y^2$$
$$\times \alpha^2\eta'(x)\eta^{(3)}(x) + y^2\alpha^2(6\eta''^2(x) - q\eta^{(4)}(x))) + 2\eta^4(x)(12(7 + 12\alpha^2\eta'^2(x))\eta''(x)$$
$$+ 27q\alpha^2\eta''^2(x) + \alpha^2(36q\eta'(x)\eta^{(3)}(x) + y^2\eta^{(4)}(x))))] + \cdots . \tag{39}$$

Now, we can evaluate the velocity and vorticity from equation (31). From the two-dimensional steady Navier-Stokes equations, introducing the stream function ψ and vorticity ω gives the pressure terms in dimensionless form as

$$\begin{aligned} \frac{\partial p}{\partial x} &= R_e\alpha[(\frac{\partial\psi}{\partial x}\frac{\partial^2\psi}{\partial y^2}) - (\frac{\partial\psi}{\partial y}\frac{\partial^2\psi}{\partial x\partial y})] - \frac{\partial\omega}{\partial y}, \\ \frac{\partial p}{\partial y} &= R_e\alpha^3[(\frac{\partial\psi}{\partial y}\frac{\partial^2\psi}{\partial x^2}) - (\frac{\partial\psi}{\partial x}\frac{\partial^2\psi}{\partial x\partial y})] + \alpha^2\frac{\partial\omega}{\partial x}. \end{aligned} \tag{40}$$

From these equation and substituting of ψ and ω we can get the value of the pressure gradients.

5 Numerical Results and Discussion

In a two dimensional symmetric channel with both walls moving, the stream function, the velocity and pressure fields are evaluated for values of the four

dimensionless parameters, the wave number α, the amplitude ratio ϕ, Reynolds number R_e and volume flow rate q.

5.1 Velocity Field

To study the behavior of the distributions of the longitude velocity (u) for values of α, ϕ, R_e and q. Figures (2,3, 4and 5) depicts that the behavior of velocity near the channel walls and at center are not similar, also the longitude velocity take a cosine profile in all figures. Figure(2) show that by increasing α, longitude velocity field decreases in the region $y \in [-0.35, 0.35]$ and increases in rest of the region. Figure (3) illustrates the longitude velocity increases in the region $y \in [-0.35, 0.35]$ but decreases in the other region as ϕ increases. Figure (4) illustrates the longitude velocity increases in the region $y \in [-0.45, 0.45]$ but decreases in the other region as R_e increases. The velocity for the flow rate q is plotted in figure(5) . It is found that the velocity field increases with an increase in the flow rate.
To study the behavior of the distributions of the vertical velocity v for several values of α, ϕ, R_e and q. Figures (6, 7 and 8) illustrate the velocity field increases with the increase of (α, R_e and q) in the region $y \in [-0.8, 0]$ while velocity field decreases in the region $y \in [0, 0.8]$. In figure (9) for the region $y \in [-0.8, 0]$ we show that the velocity field near to the wall decreases as ϕ increases while increases in the other region, but vice versa in the region $y \in [0, 0.8]$.
Our results are compared with those obtained by Mekheimer[10] in the case of no magnetic field and couple stresses. Such a comparison is illustrated in tables (1) and(2) and figure (10), where we notice a light difference between the two solutions in the middle of the channel and coincide near to the walls of the channel.

y	u(x,y) present work	u(x,y) Mekheimer[10]	|error|
-0.7	-1	-1	0
-0.5	0.2596056825	0.2594752187	0.0001304638
-0.3	1.0991139256	1.0991253644	0.0000114389
-0.1	1.5187993716	1.5189504373	0.0001510658
0.1	1.5187993716	1.5189504373	0.0001510658
0.3	1.0991139256	1.0991253644	0.0000114389
0.5	0.2596056825	0.2594752187	0.0001304638
0.7	-1	-1	0

Table 1: Comparison of longitude velocity distribution for present work when α=0.01, R_e = 0.01 and work obtained by Mekheimer[10] for fixed values of ϕ=0.3, q=0.5

y	u(x,y) present work	u(x,y) Mekheimer[10]	|error|
-0.9	-1	-1	0
-0.7	-0.3415306332	-0.3415637860	0.0000331528
-0.5	0.1522789412	0.1522633744	0.0000155667
-0.3	0.4814651075	0.4814814815	0.0000163740
-0.1	0.6460521253	0.6460905350	0.0000384097
0.1	0.6460521253	0.6460905350	0.0000384097
0.3	0.4814651075	0.4814814815	0.0000163740
0.5	0.1522789412	0.1522633744	0.0000155667
0.7	-0.3415306332	-0.3415637860	0.0000331528
0.9	-1	-1	0

Table 2: Comparison of longitude velocity distribution for present work when α=0.01, R_e = 0.01 and work obtained by Mekheimer[10] for fixed values of ϕ=0.1, q=0.1

5.2 Pressure Field

Figures (11,12 and 14) illustrate that in the wider part of the channel $x \in [0, 0.6]$ and [0.9, 1.2] the pressure gradient is relatively small, that is, the flow can easily pass without imposition of large pressure gradient. Where, in a narrow part of the channel $x \in [0.6, 0.9]$ a much larger pressure gradient is required to maintain the same flux to pass it, especially for the narrowest position near $x = 0.8$. This is in well agreement with the physical situation. Also from these two figures we observe the effect of α and q on the pressure gradient, for fixed values of the other parameters, where the amplitude of $\frac{\partial p}{\partial x}$ increases with increasing of α and q, while it decrease as ϕ increases, and for small value of $\phi = 0.1$ (small amplitude of the channel wave) a small varies on the pressure gradient, as expected. The effects of R_e on the pressure distribution along the wall are illustrated in figure (13). When R_e is small, the pressure on the wall is negative at all the cross section of the channel. The distribution along the wall is slightly antisymmetric about the midsection. As R_e increases, the magnitudes of the maximum and minimum pressures, increase. Also a nearly symmetric distribution along the wall is found. At R_e is large,the pressure on the wall is negative at the contracting part of the channel and is positive at the dilating part. Owing to the antisymmetrical pressure distribution the flow is given the energy equal to the pressure work done by the motion of the wall in a relatively greater degree than in the symmetric pressure distribution case, and this energy is consumed in the flow as the stress work caused by the viscosity of fluid.
In the figures (15, 16, 17 and 18) the distribution is slightly antisymmetric about the midsection. The pressure vanishes at the center line $y = 0$ and

other two points for y (critical points, where the sign of the pressure value change) which are different according to the parameter values . In all figures the pressure $\frac{\partial p}{\partial y}$ takes negative and positive values in both regions of the half channel and behaves as a sinusoidal wave across the channel. Finally the effect of the problem parameter are illustrated in these figures , where the $\frac{\partial p}{\partial x}$ amplitude increases as the wave number α , flow rate q , amplitude ratio ϕ and R_e increases, the variance of this amplitude wave is clear for R_e and have a great influence on the pressure.

5.3 Trapping

An interesting phenomenon of peristaltic motion in the wave frame is trapping which is basically the formation of an internally circulating bolus of fluid by closed streamlines. This trapped bolus is pushed ahead with the peristaltic wave. Figure (19) illustrates the streamline graphs for different values of the wave number α. It is observed that the size of trapped bolus increases by increasing the wave number. It is also observed that the number of trapped bolus also increases by increasing the wave number. Figure (20) shows the effects of the amplitude ratio ϕ, with a given fixed set of the other parameters. By increasing ϕ the size and the number of bolus increases. To see the effects of Reynolds number R_e, figure (21) is plotted. It is observed that for small values of R_e the bolus appears in the center region and moves towards left and increases in size and number as R_e increases. Figure (22) depicts that the size and number of trapped bolus increases by increasing q.

6 Conclusions

The conclusions in this paper are summarized as follows.

1. The Adomian Decomposition Method(ADM) is able to solve problems of peristaltic transport without any approximation on the magnitudes of the wave number (α), amplitude ratio (ϕ) and Reynolds number (R_e).

2. Among the geometrical conditions of the peristaltic wave, amplitude ratio (ϕ) is supposed to be an important factor which dominates the flow field.

3. For R_e is small, the pressure on the wall is negative at all the cross section of the channel. The distribution along the wall is slightly antisymmetric about the midsection.. At R_e is large,the pressure on the wall is negative at the contracting part of the channel and is positive at the dilating part.Owing to the antisymmetrical pressure distribution the flow is given the energy equal to the pressure work done by the motion of the wall in a relatively greater degree than in the symmetric pressure distribution

case, and this energy is consumed in the flow as the stress work caused by the viscosity of fluid.

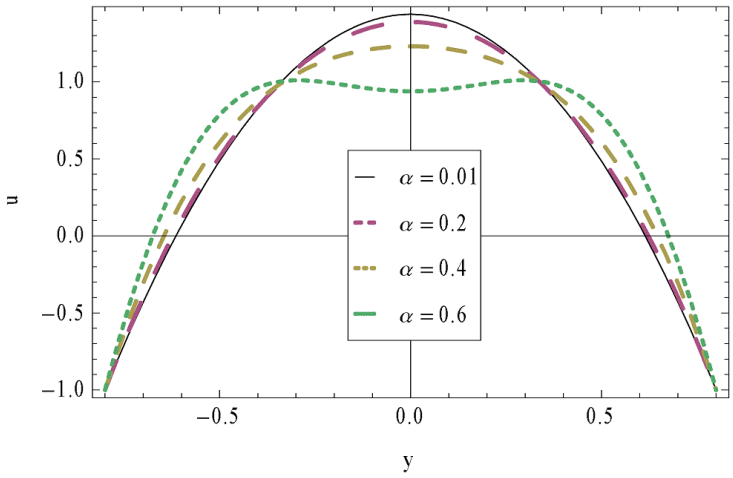

Figure 2: longitude velocity distribution for different values of α and ϕ=0.2,R_e=0.1,q=0.5

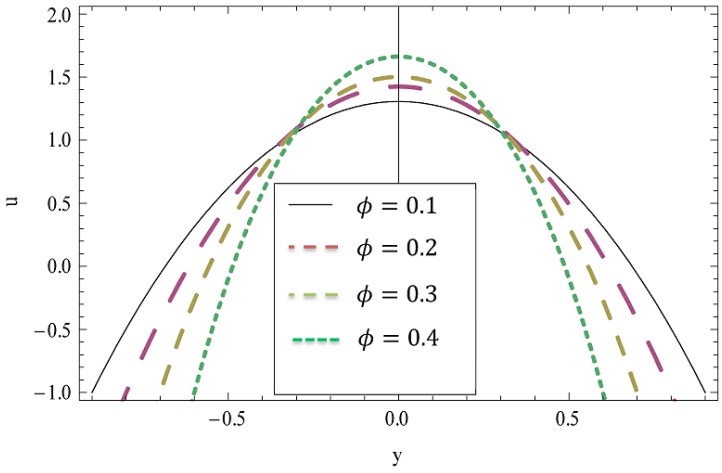

Figure 3: longitude velocity distribution for different values of ϕ and α=0.2,R_e=0.1,q=0.5

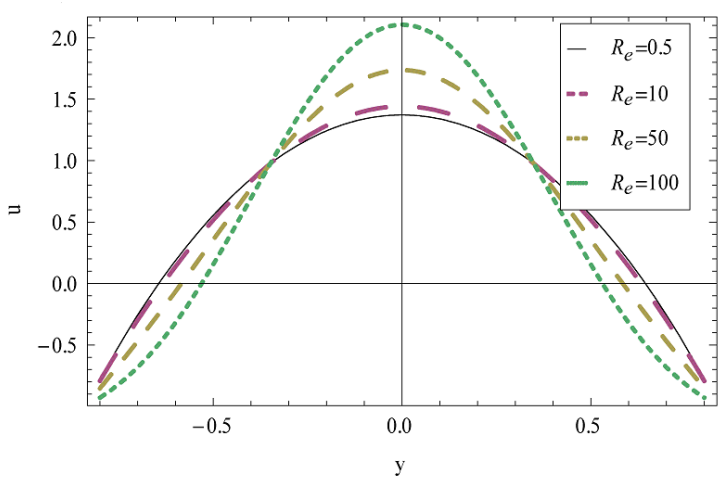

Figure 4: longitude velocity distribution for different values of R_e and α=0.2,ϕ=0.2, q=0.5

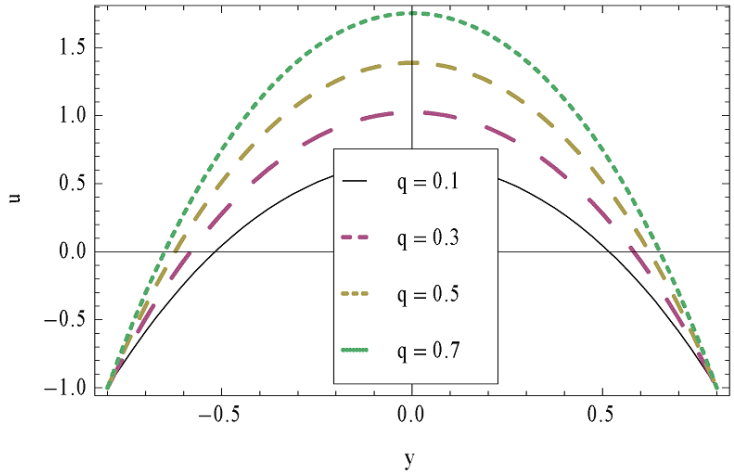

Figure 5: longitude velocity distribution for different values of q and α=0.2,ϕ=0.2, R_e=0.1

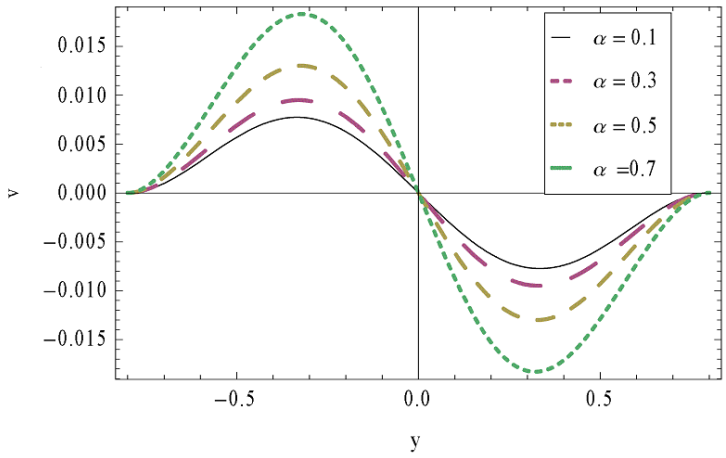

Figure 6: vertical velocity distribution for different values of α and ϕ=0.2, R_e=0.1,q=0.5

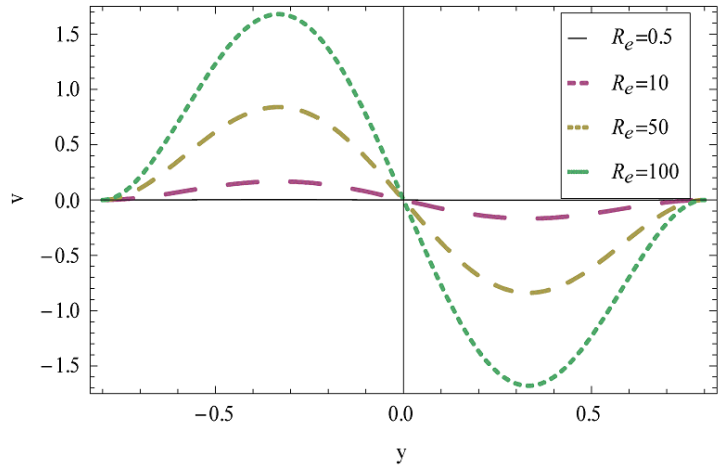

Figure 7: vertical velocity distribution for different values of R_e and α=0.2,ϕ=0.2,q=0.5

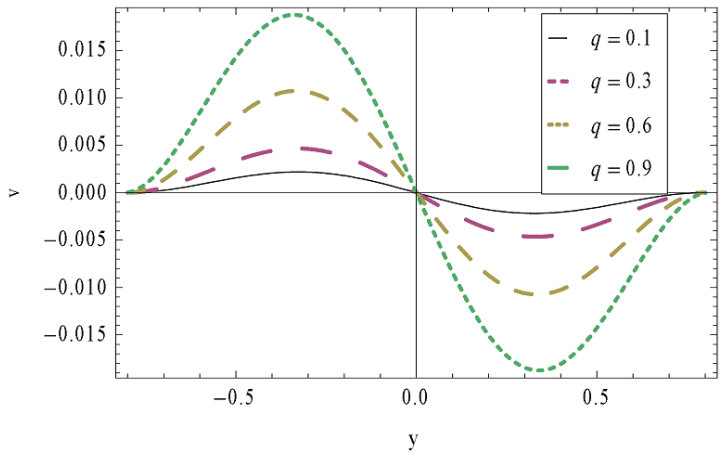

Figure 8: vertical velocity distribution for different values of q and α=0.2,ϕ=0.2,R_e=0.1

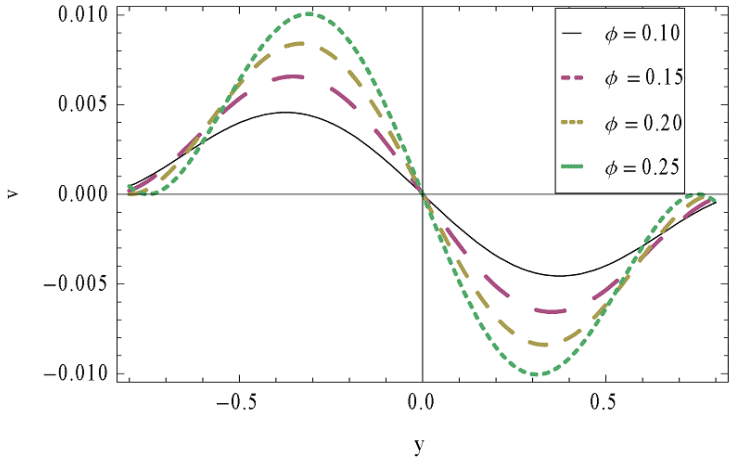

Figure 9: vertical velocity distribution for different values of ϕ and α=0.2,R_e=0.1,q=0.5

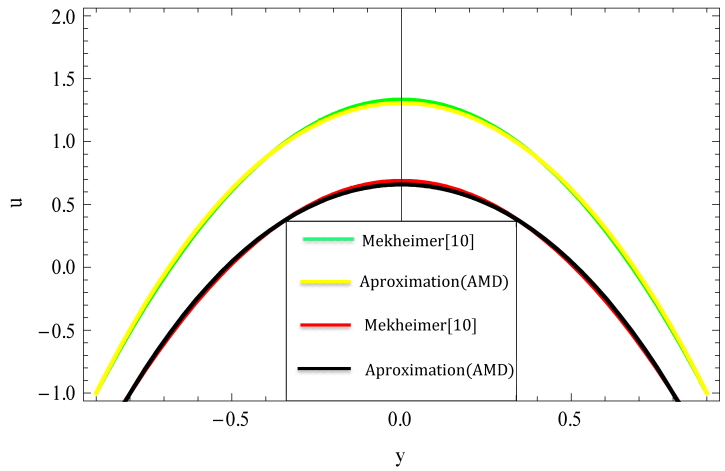

Figure 10: Comparison between present method($\alpha \neq 0$, $R_e \neq 0$) and result obtained by Mekheimer[18]. (a) ϕ =0.1, q=0.5; (b) ϕ=0.2,q=0.1

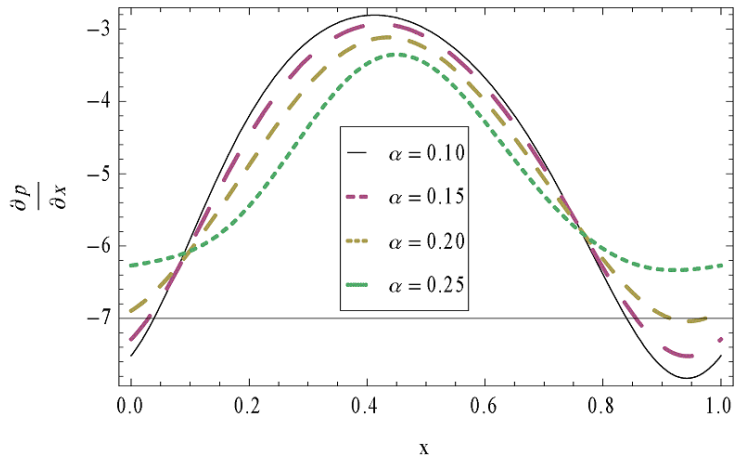

Figure 11: Variation of pressure gradient ($\frac{\partial p}{\partial x}$) for different values o f α and ϕ=0.2,R_e=0.1,q=0.5

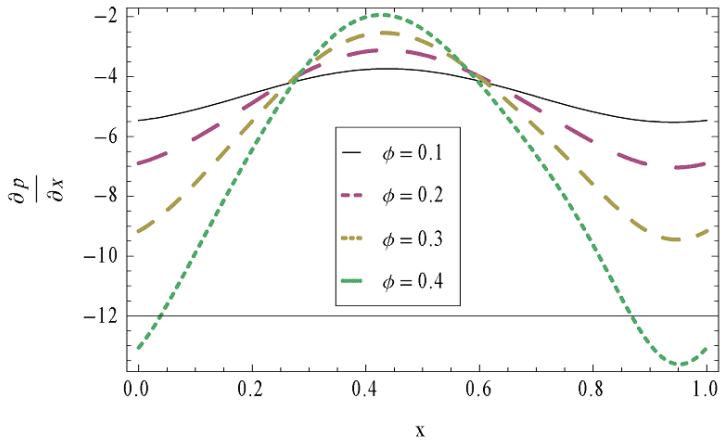

Figure 12: Variation of pressure gradient ($\frac{\partial p}{\partial x}$) for different values o f ϕ and α=0.2,R_e=0.1,q=0.5

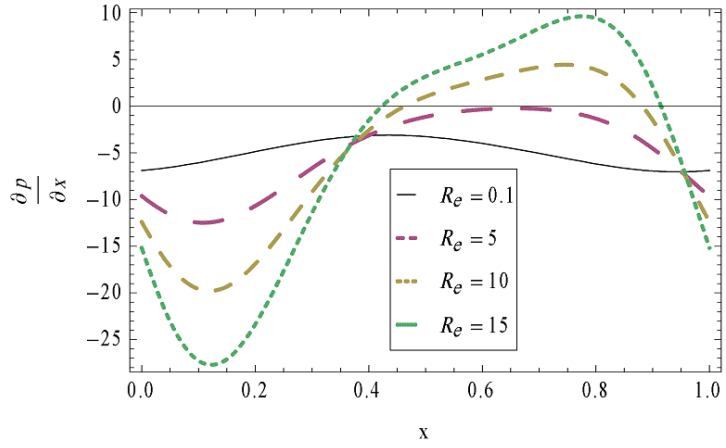

Figure 13: Variation of pressure gradient ($\frac{\partial p}{\partial x}$) for different values o f R_e and α=0.2,ϕ =0.2,q=0.5

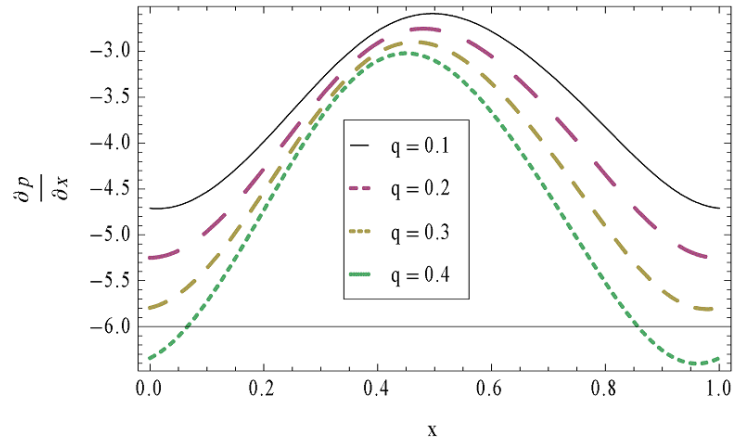

Figure 14: Variation of pressure gradient ($\frac{\partial p}{\partial x}$) for different values o f $q$and α=0.2,ϕ =0.2,R_e=0.1

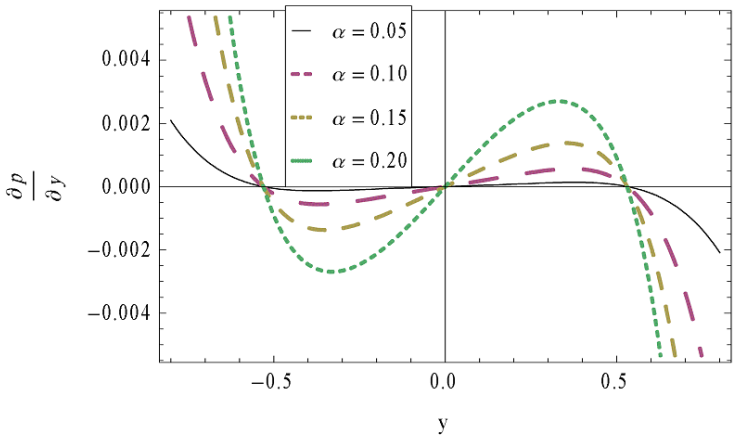

Figure 15: Variation of pressure gradient ($\frac{\partial p}{\partial y}$) for different values o f α and ϕ=0.2,R_e=0.1,q=0.1

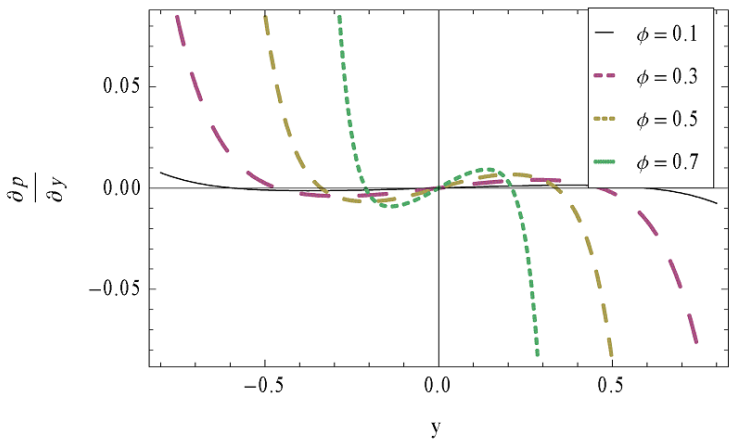

Figure 16: Variation of pressure gradient $(\frac{\partial p}{\partial y})$ for different values o f ϕ and α=0.2,R_e=0.1,q=0.1

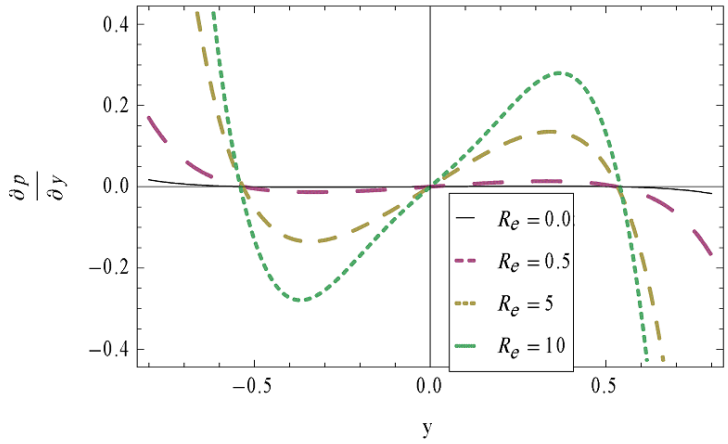

Figure 17: Variation of pressure gradient $(\frac{\partial p}{\partial y})$ for different values o f R_e and α=0.2,ϕ =0.2,q=0.5

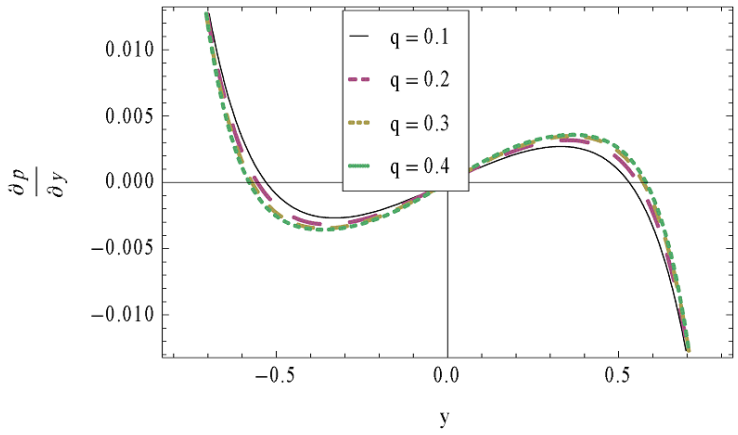

Figure 18: Variation of pressure gradient ($\frac{\partial p}{\partial y}$) for different values o f $q$and α=0.2,ϕ =0.2,R_e=0.1

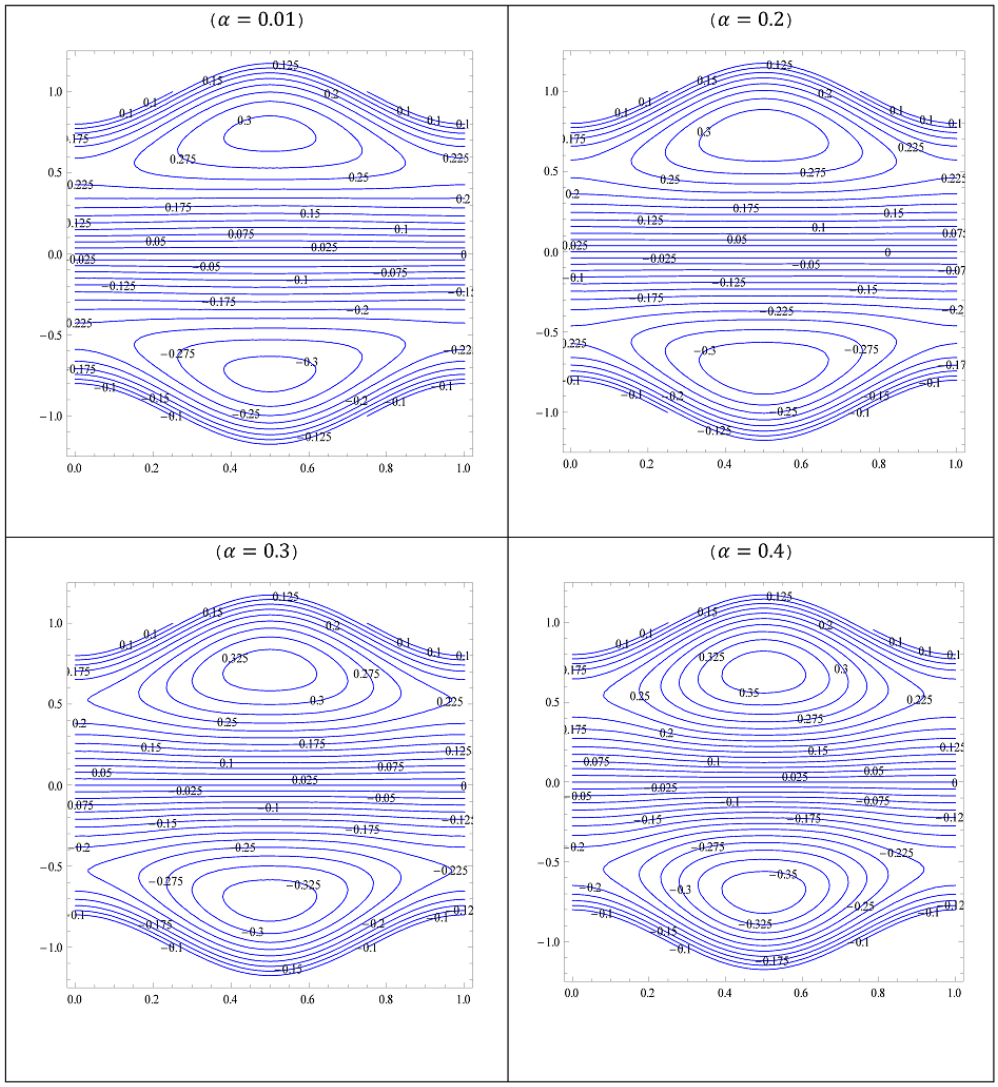

Figure 19: Streamlines for different values of (α=0.01,0.2,0.3,0.4) the other parameters are (ϕ=0.2,R_e=0.1,q=0.1).

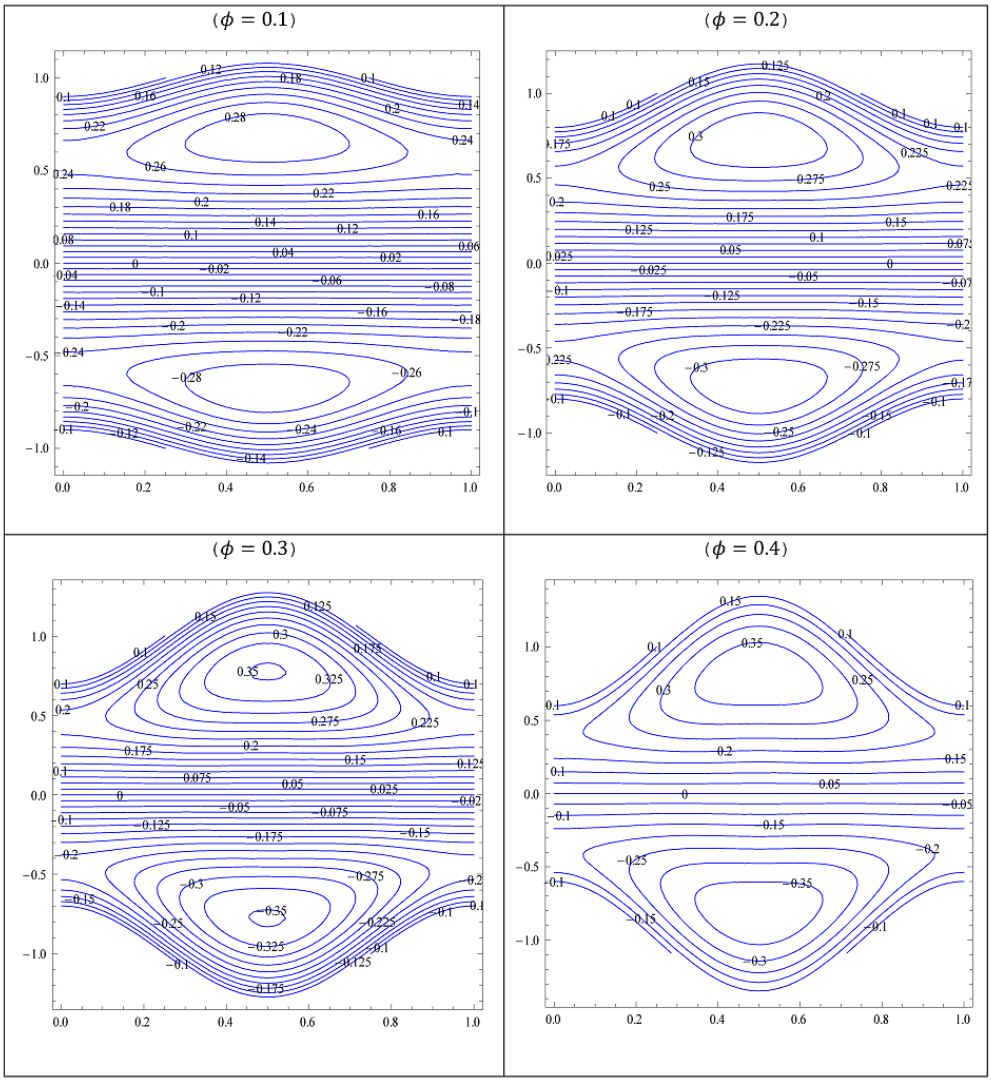

Figure 20: Streamlines for different values of (ϕ=0.1,0.2,0.3,0.4) the other parameters are (α=0.2,R_e=0.1,q=0.1).

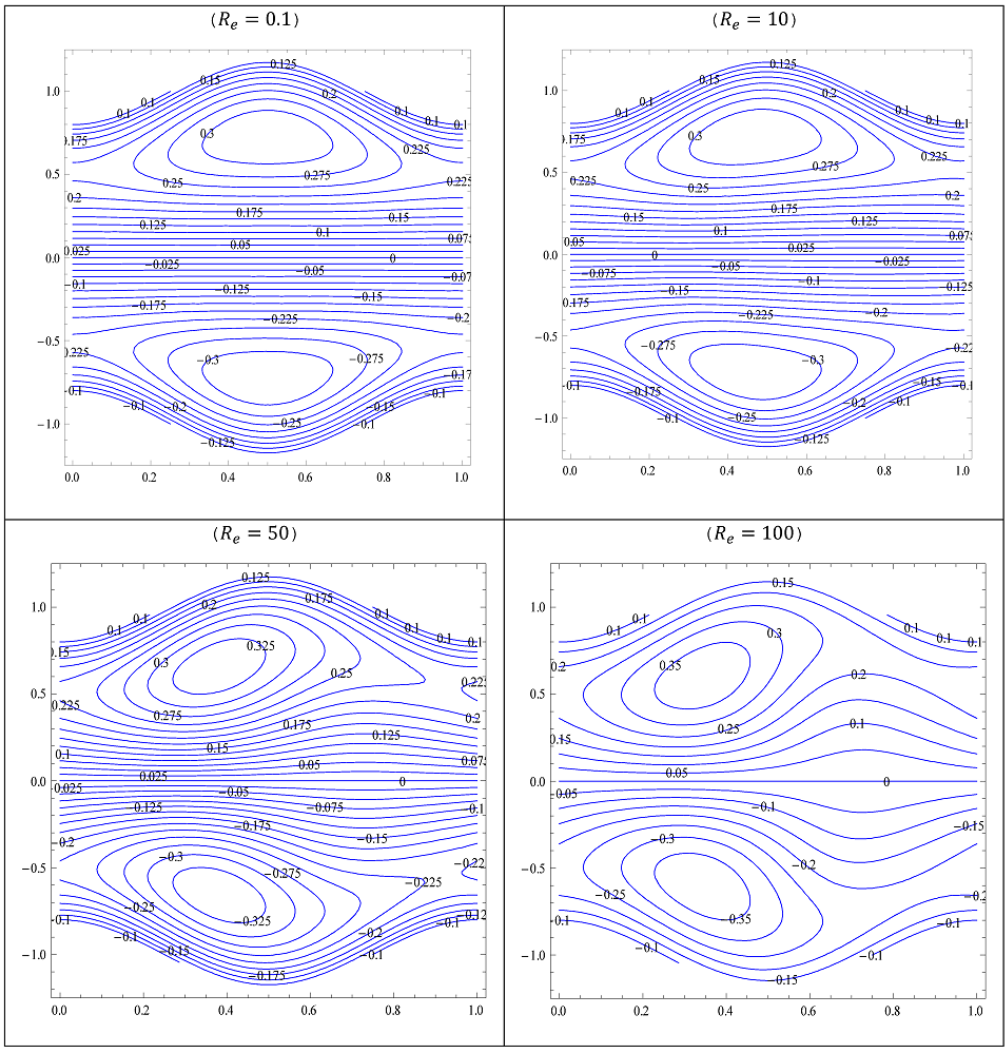

Figure 21: Streamlines for different values of (R_e=0.1,10,50,100) the other parameters are (α=0.2,ϕ=0.2,q=0.1).

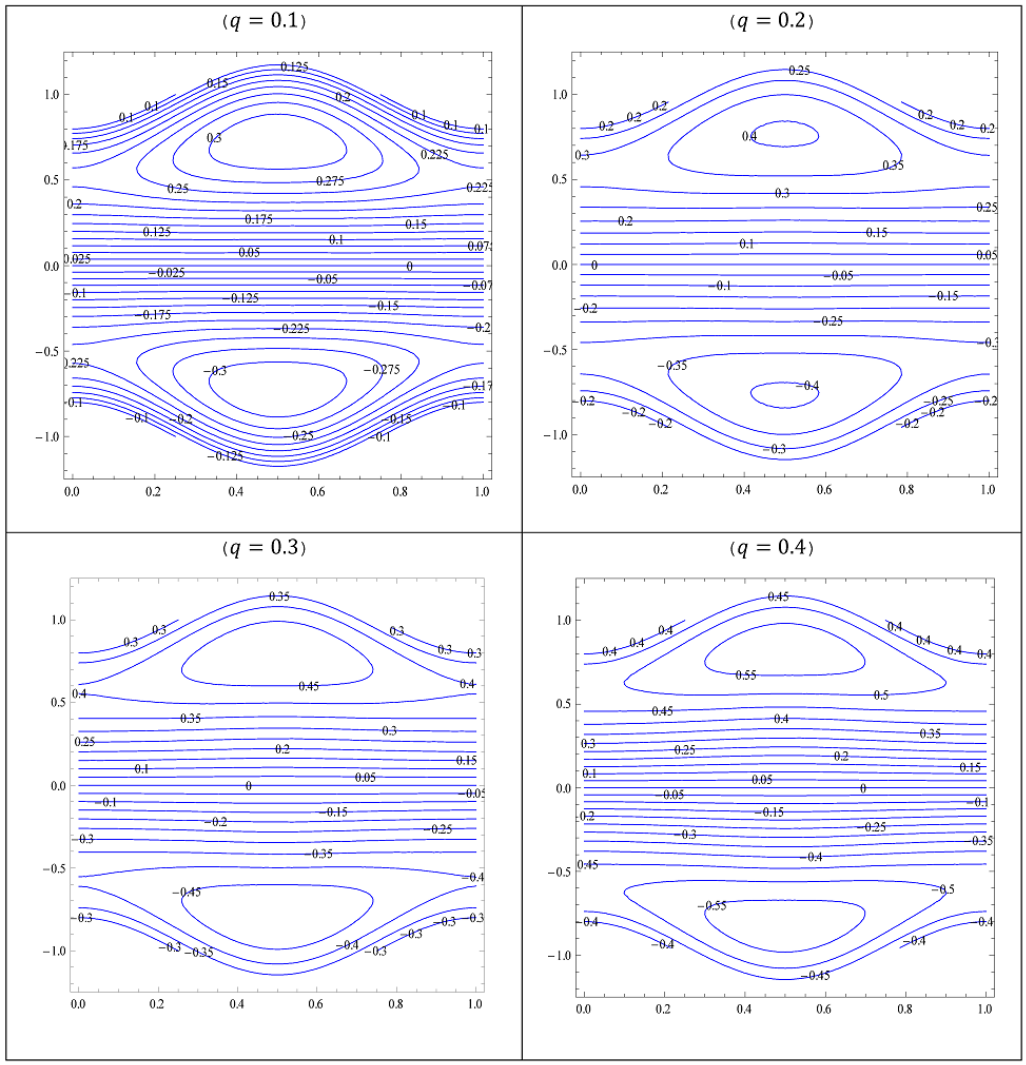

Figure 22: Streamlines for different values of $(q = 0.1, 0.2, 0.3, 0.4)$ the other parameters are $(\alpha = 0.2, \phi = 0.2, R_e = 0.1)$.

Acknowledgements: The authors wish to express their sincere thanks to the honorable referees for their valuable comments and suggestions which led to definite improvement of the paper.

References

[1] M.Y. Jaffrin and A.H. Shapiro, Peristaltic pumping, *Annual Review of Fluid Mechanics*, 3(1971), 13-37.

[2] Y.C. Fung and C.S. Yih, Peristaltic transport, *Trans. ASME. E. J. Appl. Mech.*, 35(1968), 669-675.

[3] A.H. Shapiro, M.Y. Jaffrin and S.L. Weinberg, Peristaltic pumpuing with long wave lengths at low Reynolds number, *J. Fluid Mech.*, 37(1969), 799-825.

[4] M.Y. Jaffrin, Inertia and streamline curvature effects on peristaltic pumping, *Int. J. Engng Sci.*, 11(1973), 681-699.

[5] S.L. Weinberg, E.C. Eckstein and A.H. Shapiro, An experimental study of peristaltic pumping, *J. Fluid Mech.*, 49(1971), 461-479.

[6] M.Y. Hanin, The flow through a channel due to transversely oscillating walls, *Israel J. Tech.*, 6(1968), 67-71.

[7] K. Ayukawa, T. Kawai and M. Kimura, Streamlines and path lines in peristaltic flows at high Reynolds numbers, *Bull. Japan Soc. Mech. Engrs.*, 24(1981), 948-955.

[8] P. Tong and D. Vawter, An analysis of peristaltic pumping, *Trans. ASMEE. J. Appl. Mech.*, 39(1972), 857-862.

[9] T.D. Brown and T.K. Hung, Computational and experimental investigation of two dimensional nonlinear peristaltic flows, *J. Fluid Mech.*, 83(1977), 249-272.

[10] Kh. S. Mekheimer, Peristaltic flow of blood under effect of a magnetic field in a non uniform channels, *Appl. Math. Comput.*, 153(2004), 763-777.

[11] Kh. S. Mekheimer and Y. Abd Elmaboud, The influence of heat transfer and magnetic field on peristaltic transport of a Newtonian fluid in a vertical annulus, *Physics Lett. A*, 372(2008), 1657-1665.

[12] Kh. S. Mekheimer, Effect of the induced magnetic field on peristaltic flow of a couple stress fluid, *Phys Let A*, 372(2008), 4271-4278.

[13] Y. Abd Elmaboud, Kh. S. Mekheimer and A. Abdellatif, Thermal properties of ocouple-stress fluid in an asymmetric channel with peristalsis, *J. Heat Transfer*, 135(4) (2013).

[14] G. Adomian, *Solving Froniter Problems of Physics: The Decomposition Method*, Kluwer Academic Publishers, Boston, (1994).

[15] G. Adomian, A review of the decomposition method in applied mathematics, *J. Math. Anal. Appl.*, 135(1988), 501-544.

[16] A.K. Khalifa, K.R. Raslan and H.M. Alzubaidi, Numerical syudy using ADM for the modified regularized long wave equation, *Applied Mathematical Modeling*, 32(2008), 2962-2972.

[17] A.M. Wazwaz, The decompostition method applied to the system of partial differential equations and reaction-diffusion Brusselator model, *Appl. Math. Comput.*, 110(2000), 251-264.

[18] H.N. Ismail, K.R. Raslan and G.S. Salem, Solitary wave solutions for the general KdV equation by Adomian decomposition method, *Appl. Math. Comput.*, 154(2004), 17-29.